

Thermoelectric Power of Dirac Fermions in Graphene

Xin-Zhong Yan^{1,2}, Yousef Romiah², and C. S. Ting²¹Institute of Physics, Chinese Academy of Sciences, P.O. Box 603, Beijing 100190, China²Texas Center for Superconductivity, University of Houston, Houston, Texas 77204, USA
(Dated: July 18, 2022)

On the basis of self-consistent Born approximation for Dirac fermions under charged impurity scatterings in graphene, the theory for calculating the thermoelectric power is developed by using the heat current-current correlation function. The advantage of the present approach is its ability to effectively treat the low doping case where the coherence process involving carriers in both upper and lower bands becomes important. We show that the low temperature behavior of the thermoelectric power as function of the carrier concentration and the temperature observed by the experiments can be successfully explained by our calculation.

PACS numbers: 73.50.Lw, 73.50.-h, 72.10.Bg, 81.05.Jw

Recent experimental observations [1, 2, 3] have revealed the unusual behavior of the thermoelectric power S as function of the carrier concentration n in graphene at low temperature. Near zero carrier concentration, the observed result of S explicitly departs from the formula $S = \frac{1}{n} \frac{dP}{dT}$ given by the semiclassical Boltzmann theory [4] with n as the number of charge carriers per unit area. Instead of diverging at $n = 0$, S varies dramatically but continuously with changing sign as n varying from hole side to electron side. Although there exists phenomenological explanations on this problem [1, 5], a microscopic theory of the thermoelectric power of Dirac fermions in graphene is still lacking.

It has well established that the charged impurities in graphene are responsible for the carrier density dependences of the electric conductivity [6, 7, 8] and the Hall coefficient [15] as measured in the experiments by Novoselov et al. [9]. In the present work, based on the conserving approximation within the self-consistent Born approximation (SCBA), we develop the theory for the thermoelectric power S of the Dirac fermions in graphene using the heat current-current correlation function under the scatterings due to charged impurities. This approach has been proven to be effective in treating the transport property of graphene at low carrier density [8, 15], where the coherence between the upper and lower bands is automatically taken into account. It is the coherence which yields finite conductivity at very low carrier density. We calculate the thermoelectric power as function of carrier concentration at low temperature and compare with the experimental measurements [1, 2, 3]. We show that the experimental observations can be explained by the present calculation.

We start with description of the electrons in graphene. At low carrier concentration, the low energy excitations of electrons in graphene can be viewed as massless Dirac fermions [10, 11, 12, 13] as being confirmed by recent experiments [9, 14]. Using the Pauli matrices σ_x 's and σ_y 's to coordinate the electrons in the two sublattices (a and b) of the honeycomb lattice and two valleys (1 and 2) in

the first Brillouin zone, respectively, and suppressing the spin indices for brevity, the Hamiltonian of the system is given by

$$H = \sum_{\mathbf{k}} \sum_{\alpha} v_{\mathbf{k}} \hat{c}_{\mathbf{k}\alpha}^\dagger \hat{c}_{\mathbf{k}\alpha} + \frac{1}{V} \sum_{\mathbf{k}\mathbf{q}} \sum_{\alpha} V_{\alpha}(\mathbf{q}) \hat{c}_{\mathbf{k}\alpha}^\dagger \hat{c}_{\mathbf{k}-\mathbf{q}\alpha} \quad (1)$$

where $\hat{c}_{\mathbf{k}} = (\hat{c}_{\mathbf{k}\alpha 1}^\dagger; \hat{c}_{\mathbf{k}\beta 1}; \hat{c}_{\mathbf{k}\alpha 2}; \hat{c}_{\mathbf{k}\beta 2})$ is the fermion operator, $v = 5.86 \text{ eV}\text{\AA}$ is the velocity of electrons, V is the volume of system, and $V_{\alpha}(\mathbf{q})$ is the electron-impurity interaction. Here, the momentum \mathbf{k} is measured from the center of each valley with a cutoff $k_c = 3a$ (with $a = 2.4 \text{ \AA}$ the lattice constant), within which the electrons can be regarded as Dirac particles. By neglecting the intervalley scatterings that are unimportant here, $V_{\alpha}(\mathbf{q})$ reduces to $n_i(\mathbf{q})v_0(\mathbf{q})/v_0(0)$ with $n_i(\mathbf{q})$ and $v_0(\mathbf{q})$ as respectively the Fourier components of the impurity density and the electron-impurity potential. For the charged impurity, $v_0(\mathbf{q})$ is given by the Thomas-Fermi type

$$v_0(\mathbf{q}) = \frac{2e^2}{(q + q_{TF})} \exp(-qR_i) \quad (2)$$

where $q_{TF} = 4k_F e^2/v$ is the TF wavenumber, k_F is Fermi wavenumber, ϵ_0 is the effective dielectric constant, and R_i is the distance of the impurity from the graphene layer. (In terms of the carrier density n , k_F is given by $k_F = \sqrt{2n}$. The parameter ρ defined as the doped carriers per carbon atom is related to n via $\rho = 3a^2 n/4$.) This model has been successfully used to study the electric conductivity [8] and the Hall coefficient [15]. As in the previous calculation, we here set $R_i = 0$ and the average impurity density as $n_i = 1:15 \times 10^{13} \text{ \AA}^{-2}$.

Under the SCBA [see Fig. 1(a)] [16, 17], the Green function $G(\mathbf{k};!) = [i + v_{\mathbf{k}} \hat{c}_{\mathbf{k}}^\dagger \hat{c}_{\mathbf{k}} - \Sigma(\mathbf{k};!)]^{-1}$, $g_0(\mathbf{k};!) + g_c(\mathbf{k};!) \hat{c}_{\mathbf{k}}^\dagger \hat{c}_{\mathbf{k}}$ and the self-energy $\Sigma(\mathbf{k};!) = \rho_0(\mathbf{k};!) + \rho_c(\mathbf{k};!) \hat{c}_{\mathbf{k}}^\dagger \hat{c}_{\mathbf{k}}$ of the single particles are de-

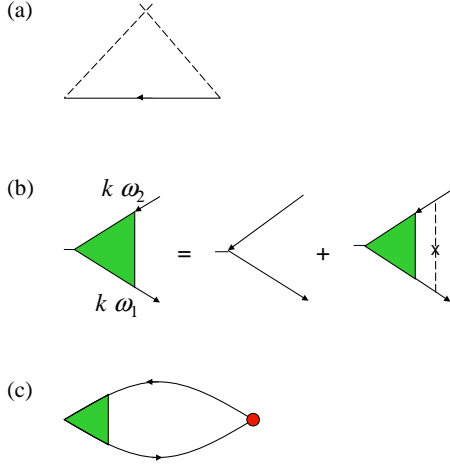


FIG. 1: (color online) (a) Self-consistent Born approximation for the self-energy of the single Dirac fermion. (b) Current vertex with impurity insertions. (c) Heat current-current correlation function. The red solid circle denotes the heat current vertex.

term ined by coupled integral equations [8]:

$$g_0(k;!) = \frac{n_i}{V} \sum_{k^0} v_0^2 (\mathbf{j} \cdot \mathbf{k}^0) g_0(k^0;!) \quad (3)$$

$$g_c(k;!) = \frac{n_i}{V} \sum_{k^0} v_0^2 (\mathbf{j} \cdot \mathbf{k}^0) g_c(k^0;!) \hat{k} \cdot \hat{k}^0 \quad (4)$$

$$g_0(k;!) = \frac{1}{2} [g_+(k;!) + g_-(k;!)] \quad (5)$$

$$g_c(k;!) = \frac{1}{2} [g_+(k;!) - g_-(k;!)] \quad (6)$$

where $g_{\pm}(k;!) = [1 + v \mathbf{k} \cdot \mathbf{k}^0 g_0(k^0;!) \pm g_c(k^0;!)]^{-1}$ with the chemical potential, \hat{k} is the unit vector in k direction, and the frequency $!$ is understood as a complex quantity. Here g_+ (g_-) [g_c (g_c)] can be viewed as the upper (lower) band Green function.

We now consider the thermal transport. The (particle) current J_1 and heat current J_2 operators are defined as

$$J_1 = \frac{1}{V} \sum_{\mathbf{k}} v \cdot \mathbf{k} z \sim \mathbf{k}$$

$$J_2 = i v \sum_{\mathbf{k}} \frac{1}{V} \sum_{k^0} v_0^2 (\mathbf{j} \cdot \mathbf{k}^0) z \sim \frac{\partial}{\partial t} \mathbf{k} :$$

They correspond respectively to the forces $X_1 = T^{-1} r(\epsilon)$ and $X_2 = r(1=T)$ with T as the temperature and ϵ the external electric potential. According to the linear response theory, the thermo-electric power is given by $S = L^{21} = e T L^{11}$ where the linear response coefficients L are obtained from the correlation function (7) by

$$L = T \lim_{! \rightarrow 0} \text{Im} \chi(+) = :$$

For the bosonic Matsubara frequency ω_n , $\chi(\omega_n)$ reads

$$\chi(\omega_n) = \frac{1}{V} \sum_{\mathbf{k}} \int_0^{\beta} d\tau e^{i \omega_n \tau} \text{Tr} [J_x(\tau) J_x(0)]$$

with $\beta = 1/T$. The quantity $L^{11} = T^{-2} \sigma$ is related to the electric conductivity σ which we have obtained in our previous work [15].

Within the SCBA, the correlation function is determined with the vertex corrections. A common vertex $v_x(k;!_1;!_2)$ given as the ladder diagrams in Fig. 1(b) can be factorized out. $v_x(k;!_1;!_2)$ is expanded as [15]

$$v_x(k;!_1;!_2) = \sum_{j=0}^{\infty} Y_j(k;!_1;!_2) A_j^x(\hat{k})$$

where $A_0^x(\hat{k}) = v_x$, $A_1^x(\hat{k}) = v_x \hat{k}_x$, $A_2^x(\hat{k}) = v_x \hat{k}_x^2$, $A_3^x(\hat{k}) = v_x \hat{k}_x^3$, and $Y_j(k;!_1;!_2)$ are determined by four-coupled integral equations [8]. In the following, since the heat current-current correlation function will be analyzed for the case of $!_1 = ! - i0^+$ and $!_2 = ! + i0^+$, we here need to write out the relevant equations for this case. For brevity, we denote $Y_j(k;!_1;!_2)$ simply as $Y_j(k;!)$. To write in a compact form, we define the 4-dimensional vector $Y^t = (Y_0; Y_1; Y_2; Y_3)$ (where the superscript t implies transpose), and the matrices,

$$U(k;k^0) = n_i v_0^2 (\mathbf{j} \cdot \mathbf{k}^0) \begin{pmatrix} 0 & 1 & 0 & 0 \\ 0 & \cos \theta & 0 & 0 \\ 0 & 0 & \cos \theta & 0 \\ 0 & 0 & 0 & \cos 2\theta \end{pmatrix}$$

where θ is the angle between k and k^0 , and

$$M(k;!) = \begin{pmatrix} 0 & 1 \\ g_0 & g_c \\ g_c & g_0 \\ g_0 & g_c \\ g_c & g_0 \end{pmatrix}$$

where g_{\pm} are complex conjugate of $g_{0,\pm} = g_{0,\pm}(k;!^+)$. The equation determining $Y(k;!)$ is then given by

$$Y(k;!) = Y_0 + \frac{1}{V} \sum_{k^0} U(k;k^0) M(k^0;!) Y(k^0;!) \quad (7)$$

with $Y_0^t = (1; 0; 0; 0)$.

We need to calculate the heat current-current correlation function χ^{21} and then the coefficient L^{21} . Within the SCBA to the single particles, the correlation function χ^{21} is determined by the diagram given by Fig. 1(c), which is a conserving approximation. From Fig. 1(c), we have

$$\chi^{21}(\omega_n) = \frac{2v^2 T}{V} \sum_{\mathbf{k}, \mathbf{k}^0} \text{Tr} [v_x G(k;!_n) v_x G(k;!_n + i\omega_n)] \quad (8)$$

where the factor 2 is due to the spin degeneracy, $i\omega_n$ (the fermionic Matsubara frequency) in front of the trace Tr operation comes from the heat vertex. The difference between $L^{21}(\omega)$ and $L^{11}(\omega)$ is there is the factor $i\omega_n$ in the above expression. According to the standard procedure [18], by performing the analytical continuation $i\omega_n \rightarrow \omega + i0$ and taking the limit $\omega \rightarrow 0$, one then gets L^{21} in terms of the integral with respect to the real frequency. At low temperature, since the contribution to the integral comes from a small region around $\omega = 0$, one can carry out the integration and get $L^{21} = 2T^3 \rho = 3e^2$. Here ρ is defined as $2\rho = dP(\omega; \mu^+) = d\sum_{j=0}^{\infty} \omega_j$ with $P(\omega; \mu^+)$ given by

$$P(\omega; \mu^+) = \frac{8v^2 e^2 X}{V} \sum_{kj} M_{0j}(\mathbf{k}; \omega) Y_j(\mathbf{k}; \omega) \quad (9)$$

Clearly, the quantity ρ is involved with the frequency derivative of the Green function $g_{0,c}(\mathbf{k}; \omega)$ and $y_j(\mathbf{k}; \omega)$'s. The functions $\partial g_{0,c}(\mathbf{k}; \omega) = \partial \omega$ and $\partial y_j(\mathbf{k}; \omega) = \partial \omega$ are determined by a number of coupled integral equations which can be obtained from Eqs. (3)–(6) and (7). To calculate the thermoelectric power S , we need to solve not only Eqs. (3)–(6) and (7) but also their frequency derivative at $\omega = 0$. By using the results for L^{21} and L^{11} , the expression for the thermoelectric power is obtained as

$$S = \frac{2T}{3e} \rho \quad (10)$$

in form all the same as the Mott relation [4].

We have numerically solved the integral equations for determining the functions $g_{0,c}(\mathbf{k}; \omega)$, $y_j(\mathbf{k}; \omega)$, $\partial g_{0,c}(\mathbf{k}; \omega) = \partial \omega$ and $\partial y_j(\mathbf{k}; \omega) = \partial \omega$ at $\omega = 0$ for various carrier concentrations. With these results, the quantity ρ and the thermoelectric power S can be calculated accordingly. Shown in Fig. 2 is the obtained quantity ρ as a function of the carrier concentration. The circles on the curve represent the numerical data points. ρ increases with μ monotonically and is odd with respect to (electron) $\mu -$ (hole). A notable feature is that ρ varies dramatically within a narrow region μ_0 to μ_0 with $\mu_0 = 7 \times 10^5$. Out of this region, the magnitude of ρ increases with a slower rate as μ increasing. The inset in Fig. 2 shows the electric conductivity at low carrier concentration. The green circles are the interpolations. The minimum conductivity so determined is $3.5 e^2/h$ close to the experimental data $4 e^2/h$. The dot-dashed line represents the extrapolation of ρ from large μ . By carefully looking at the behavior of ρ , we find that ρ starts to depart from the linearity at approximately the same μ_0 below which ρ decreases slower as μ decreasing.

At low temperature, both ρ and S are independent of T . Therefore, S is a linear function of T at low T . Shown in Fig. 3 is the numerical result for $S=T$ (red solid line with circles) as a function of the carrier concentration and the comparison with the experimental measurements (symbols) by three groups [1, 2, 3]. Within the

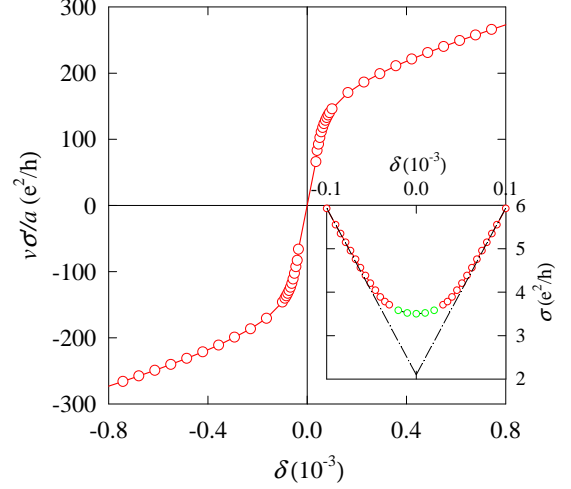


FIG. 2: (color on line) Zero frequency derivative of the current-current correlation function as function of the carrier concentration μ . The red circles denote the numerical data points. Inset: The electric conductivity σ at low carrier concentration. The green circles are the interpolations and the dot-dashed line is the extrapolation of the linear ρ in large μ .

same narrow region μ_0 to μ_0 , the calculated $S=T$ varies drastically from the maximum at μ_0 to the minimum at μ_0 . Out of this region, the magnitude of $S=T$ decreases monotonically with μ . A gain, $S=T$ is an odd function of μ . Clearly, the present calculation can capture the main feature of the experimental data. For the magnitude of $S=T$, there are obvious differences between the experimental results. This may be caused by the impurity distributions in samples treated by different experiments. It has been shown that the magnitude of S has a relatively sensitive dependence on the distance R_i of the impurities from the graphene layer [5].

The features of ρ and S may be qualitatively explained by analyzing the behavior of ρ as function of μ . Recall $\rho = P(\omega; \mu^+) = 2\sum_{j=0}^{\infty} \omega_j + 2e^2 = h \rho$. ρ is actually the functional of the Green function G and the impurity potential v_0 , both of latter two depending on μ or the chemical potential μ . If the dependence of v_0 is neglected, then one gets ρ from $d\rho = d\rho$. Based on such a consideration, it has been illustrated in Ref. 1 that the calculated S from the experimental results for μ is in overall agreement with experiment. Theoretically, at large carrier concentration, the system can be approximately described by the one band Green function, e.g., g_+ for electron doping. This is equivalent to the Boltzmann treatment to μ . On the other hand, the Boltzmann theory gives rise to a linear behavior of ρ down to very low μ close to 0. By the present formalism, however, there exists coherence between the states of upper and lower bands [19] at very low doping because the single particle energy levels are broadened under the impurity

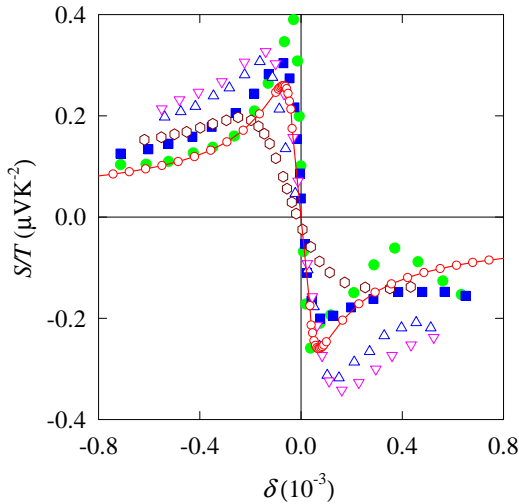


FIG. 3: (color online) Linear-T dependence coefficient S/T of thermoelectric power as function of the electron doping concentration δ . The present calculation (solid line with circles) is compared with the experimental data in Ref. 1 (solid circles at temperature $T = 150$ K and solid squares at $T = 300$ K), Ref. 2 (hexagons at $T = 255$ K), and Ref. 3 (up triangles at $T = 160$ K and down triangles at $T = 280$ K).

scatterings. The coherence is taken into account through the Green functions g in the present formalism. At $\delta = 0$, the coherence may be considered as setting in. As δ further decreases, the Fermi level gets close to the lower band and the coherence effect becomes significant. As a result, there is the minimum electric conductivity at $\delta = 0$. As seen from the inset in Fig. 2, σ decreases slower as $\delta < 0$ being closer to zero, resulting in the rapid decreasing of S/T . The unusual behavior of S/T at low doping comes from the combination of σ and S and can be understood as the coherence effect between the upper and lower Dirac bands.

The present model can not be applied to doping close to zero. At $\delta = 0$, there is no screening to the charged impurities by the model. This is unphysical. In a real system, there must exist extra opposite charges screening the charged impurities. This screening can be neglected only when above certain doping level the screening length by the carriers is shorter than that of the extra charges. Close to $\delta = 0$, the extra screening could be taken into account in a more satisfactory model. By the present model, we cannot perform numerical calculation at $\delta = 0$ because of the Coulomb divergence of $v_0(q)$ at $q = 0$. The minimum electric conductivity is obtained by interpolation.

The thermoelectric power of graphene has also been studied recently by the semiclassical approach [5]. For ex-

plaining the experimental observed transport properties of graphene at very low doping, Hwang et al. have proposed the electron-hole puddle model [7]. By this model, the local carrier density is finite and the total conductivity is given by the average of the puddles. The unusual behavior of the thermoelectric power S is so explained by the average of the Boltzmann results of S in the puddles.

In summary, on the basis of self-consistent Born approximation, we have developed the thermoelectric power theory of Dirac fermions in graphene under the charged impurity scatterings. The current correlation functions are obtained by conserving approximation. The Green function and the current vertex correction, and their frequency derivative are determined by a number of coupled integral equations. The low-doping unusual behavior of the thermoelectric power at low temperature observed by the experiments is explained in terms of the coherence between the upper and lower Dirac bands. The present calculation for the thermoelectric power is in very good agreement with the experimental measurements.

This work was supported by a grant from the Robert A. Welch Foundation under No. E-1146, the TCSUH, the National Basic Research 973 Program of China under grant No. 2005CB623602, and NSFC under grant No. 10774171 and No. 10834011.

-
- [1] Y. M. Zuev et al, arXiv:0812.1393.
 - [2] P. Wei et al, arXiv:0812.1411.
 - [3] J. G. Checkelsky and N. P. Ong, arXiv:0812.2866.
 - [4] M. Cutler and N. F. Mott, Phys. Rev. 181, 1336 (1969).
 - [5] E. H. Hwang et al, arXiv:0902.1749.
 - [6] K. Nomura and A. H. MacDonald, Phys. Rev. Lett. 98, 076602 (2007).
 - [7] E. H. Hwang et al, Phys. Rev. Lett. 98, 186806 (2007).
 - [8] X.-Z. Yan et al, Phys. Rev. B 77, 125409 (2008).
 - [9] K. S. Novoselov et al, Nature 438, 197 (2005).
 - [10] P. R. Wallace, Phys. Rev. 71, 622 (1947).
 - [11] T. Ando et al, J. Phys. Soc. Jpn. 67, 2857 (1998).
 - [12] A. H. Castro Neto et al, Phys. Rev. B 73, 205408 (2006).
 - [13] E. McCann and V. I. Fal'ko, Phys. Rev. Lett. 96, 086805 (2006).
 - [14] Y. Zhang et al, Nature 438, 201 (2005).
 - [15] X.-Z. Yan and C. S. Ting, arXiv:0904.0959.
 - [16] E. Fradkin, Phys. Rev. B 33, 3257 (1986); 33, 3263 (1986).
 - [17] P. A. Lee, Phys. Rev. Lett. 71, 1887 (1993).
 - [18] G. D. Mahan, Many-Particle Physics (Plenum, New York, 1990) 2nd Ed. Chap. 7.
 - [19] M. Trushin and J. Schliemann, Phys. Rev. Lett. 99, 216602 (2007).